The Relationship Between Upper Mantle Anisotropic Structures Beneath California, Transpression, and Absolute Plate Motions

Minoo Kosarian[1], Paul M. Davis[1], Toshiro Tanimoto[2] and Robert W. Clayton[3]

Submitted JGR 2010

[1.] Department of Earth and Space Sciences UCLA

[2.] Department of Geological Sciences, UCSB

[3.] Seismology Laboratory, California Institute of Technology

Corresponding author pdavis@ess.ucla.edu

Abstract

We calculated SKS splitting parameters for the California Integrated Seismic Network. In southern California, we also estimated splitting in the upper 100 km using azimuthal anisotropy determined from surface waves. The inferred splitting from surface waves in the mantle lithosphere is small (on average <0.2 sec) compared with SKS splitting (1.5 sec) and obtains a maximum value (0.5 sec) in the transpressive region of the Big Bend, south of, and aligned with, the San Andreas Fault (SAF). In contrast, the SKS splitting is approximately E-W and is relatively uniform spatially either side of the Big Bend of the SAF. These differences suggest that most of the SKS splitting is generated much deeper (down to 300-400 km) than previously thought, probably in the asthenosphere. Fast directions align with

absolute plate motions (APM) in northern and southeastern California but not in southwestern California. We interpret the parallelism with APM as indicating the SKS anisotropy is caused by cumulative drag of the asthenosphere by the over-lying plates. The discrepancy in southwestern California arises from the diffuse boundary there compared to the north, where relative plate motion has concentrated near the SAF system. In southern California the relative motion originated offshore in the Borderlands and gradually transitioned onshore to the SAF system. This has given rise to smaller displacement across the SAF (160-180 km) compared with central and northern California (400-500 km). Thus, in southwestern California, the inherited anisotropy, from prior North American APM, has not yet been overprinted by Pacific APM.

Introduction

One of the effective methods to infer finite strain in the deep lithosphere-asthenosphere is the measurement of seismic anisotropy thought to be associated with the alignment of olivine crystals [Becker *et al.*, 2006a; Becker *et al.*, 2006b; Becker *et al.*, 2007a; Becker *et al.*, 2007b; Kosarev *et al.*, 1984; Savage, 1999; Silver and Chan, 1991a; Silver, 1996; Silver and Holt, 2002] The study of seismic anisotropy has several applications [Montagner, 1998]. It helps (1) to define the roots of continents and to investigate if there is coupling between the lithosphere and the rest of mantle [Becker *et al.*, 2006a; Becker *et al.*, 2006b; Becker *et al.*, 2007a; Becker *et al.*, 2007b; Montagner and Tanimoto, 1991; Silver, 1996; Silver and Holt, 2002], (2) to gain information on strain, and effects of large-scale tectonics in the upper mantle [Savage, 1999], (3) to understand the dynamics of mantle convection [Becker, 2006], and (4) to detect internal boundary layers, as seismic anisotropy is

closely related to the large-strain deformation [Karato *et al.*, 1989; Montagner, 1998; Nicolas *et al.*, 1987].

One of the challenges in interpreting anisotropy is evaluation of how much is caused by lithospheric, asthenospheric and lower mantle sources [Savage, 1999] and the time scales of anisotropic fabric formation and subsequent preservation. Inferring the origin of seismic anisotropy is non-unique [Montagner, 1998; Montagner *et al.*, 2000] and further considerations are required for its interpretation such as tectonic history. For the crust, the distribution of cracks and fractures located in the vicinity of active faults may play a major role [Crampin *et al.*, 1986]. In the deep continental lithosphere, anisotropy may be due to fossil features of past tectonic events, whereas in the asthenosphere it is more likely due to recent strain. In the upper mantle, seismic anisotropy arises primarily from strain-induced lattice-preferred orientation (LPO) of the dominant mantle minerals, primarily olivine [Montagner, 1994]. The fast polarization (ϕ) tends to align parallel to the olivine a-axes, and mantle xenoliths show anisotropy of P and S velocities of up to 7% [Savage, 1999] but other slip systems can be activated depending on pressure and hydration [Karato, 2006]. It is possible to distinguish different sources of anisotropy by using different kinds (e.g., frequencies) of data, such as surface waves and local earthquake body waves, or teleseismic waves [Becker *et al.*, 2007a; Becker *et al.*, 2007b]. Also, there is a trade-off between homogeneous anisotropic models and heterogeneous isotropic models, and there is no way to distinguish between them from long wavelength seismological observation alone [Becker *et al.*, 2007a; Becker *et al.*, 2007b] . It has been long-recognized that most parts of the earth are not only laterally heterogeneous but also anisotropic and both need to be taken into account in tomographic interpretations.

Makeyeva *et al.* [1992] discussed the concept of "frozen" anisotropy in the lithosphere, noting that the mobility of olivine crystals at temperatures below ~1100 K is low. Thus a preferred orientation of olivine can be created by deformation only at temperatures higher than ~1100 K. This threshold occurs near the thermal boundary between the lithosphere and asthenosphere, and therefore anisotropy in the lithosphere is most probably "frozen in" from the past.

For the oceanic upper mantle, anisotropy reveals a relatively simple structure, with the fast axis aligned with plate motion [Montagner and Griot-Pommera, 2000; Montagner and Guillot, 2000]. However, for continental regions, due to their complex geodynamic development and deformation, it is not as simple. The two main methods for observing anisotropy are shear wave splitting of seismic phases SKS and SKKS, and travel time variations of surface wave data [Prindle and Tanimoto, 2006; Yang and Forsyth, 2006]. SKS and SKKS waves are Earth's core phases that emerge with radial polarization, and arrive at the receiver along a near vertical path. Azimuthal anisotropy underneath the receiver temporally splits the waves depending on their polarization. Resolving anisotropy using surface wave data requires path coverage in all directions. In contrast with seismic anisotropy obtained from SKS/SKKS splitting, anisotropy derived from surface waves can be localized at depth. Both measurements can be integrated to understand tectonic processes prevailing in a given tectonic context [Yang and Forsyth, 2006]. Patterns for fast velocity axes derived from these datasets (shear wave splitting and surface wave data) may appear inconsistent as the two types of data have different depth sensitivities.

Wuestefeld *et al.* [2009] compare global shear wave splitting patterns with surface wave anisotropy and find a statistically significant correlation. However the splitting times predicted by the surface waves are found to be significantly less than those determined from

SKS splitting. They suggest that this may be a result of the different spatial averaging window of the surface waves ~1000 km compared with that of SKS splitting Fresnel zones ~100 km. In addition, horizontally traveling surface waves weight vertical averages of anisotropic parameters differently than vertically traveling body waves.

Montagner and Griot-Pommera [2000] showed that at low frequencies, and weak anisotropy, splitting parameters (dt, ϕ) are related to the surface wave 2ψ variation

$$
\begin{aligned}
\rho V_1^2 &= L + G_C \cos 2(\psi - \psi_0) + G_S \sin 2(\psi - \psi_0) \\
\rho V_2^2 &= L - G_C \cos 2(\psi - \psi_0) - G_S \sin 2(\psi - \psi_0)
\end{aligned}
\tag{1}
$$

by

$$
dt = \sqrt{C^2 + S^2}, \text{ where}
$$

$$
C = \int_0^a \sqrt{\frac{\rho}{L}} \frac{G_C}{L} dz; \quad S = \int_0^a \sqrt{\frac{\rho}{L}} \frac{G_S}{L} dz
\tag{2}
$$

$$
\phi_{fast} = \frac{1}{2} \text{atan} \left(\frac{S}{C} \right)
$$

where ρ is density, z is depth, a is the depth of anisotropy and $G_S = C_{45}$, $G_C = \frac{1}{2}(C_{55} - C_{44})$

and $L = \frac{1}{2}(C_{44} + C_{55})$ are parameters that can be determined from surface wave studies, for example, by fitting azimuthal dependence of Rayleigh phase velocities to Eq. (1). Wuestefeld *et al.* [2009] used Eq. (1) to estimate splitting from the tomographic model of Debayle et al., (2005) and found a statistically significant global correlation at wavelengths greater than about 600 km, but which breaks down at lower scales suggesting splitting takes place near the Earth's surface.

There has been considerable controversy as to how much of SKS splitting is due to absolute plate motions (APM), and how much to finite strain of the lithosphere [Silver, 1996] and whether an additional effect occurs due to mantle flow, unrelated to plate motions. For example, for southern California, Silver and Holt [2002] have suggested that an east-west

directed mantle flow might explain discrepancies between splitting directions and WSW plate motion, perhaps associated with the sinking Farallon slab. In contrast, Polet and Kanamori, [2002] have suggested fast directions are related to compressive stress.

In this paper, we present new shear-wave splitting observations for the events shown in Figure 1 measured at 126 broadband seismograph stations in southern California and 35 in central and northern California. We examine the relationship between anisotropic structures within the lithosphere and asthenosphere, and the tectonic deformation process and plate motions associated with the Californian transform boundary, and compare the results with splitting inferred from surface waves.

Data and Method

Surface Wave Analysis

The surface wave analysis is described in [Prindle and Tanimoto, 2006; Tanimoto and Prindle, 2007] in which they estimated azimuthal anisotropy in several layers including upper and lower crustal layers (0-15) km and (15-33) km, a mantle lithosphere layer (33-100 km) and an asthenospheric layer (100-150 km). Phase velocities of Rayleigh waves were calculated for various frequency bands after correcting for refraction effects that caused deviation for ray paths from the great circles to the events. They fit the data with a 2ψ variation given by

$$V = V_0 + \Delta V \cos 2(\psi - \psi_G) \tag{3}$$

where ψ is azimuth (clockwise from north) and ψ_G is the fast direction. Removal of a 4ψ term is justified for Southern California as a recent array analysis of Rayleigh waves demonstrated small amplitudes for 4ψ variation [Alvizuri and Tanimoto, 2011]. This set of

data was inverted for depth variations of anisotropy, making a simplifying assumption on the form of anisotropy that the symmetry axes of P- and S-wave velocity align in the horizontal plane and the medium has hexagonal symmetry. Under these assumptions, the formulation becomes

$$\frac{\delta V}{V} = \int \{K_S \frac{\Delta V_S}{V_S} + K_P \frac{\Delta V_P}{V_P}\} \cos\{2(\psi - \psi_G)\} dz \tag{4}$$

where $\Delta V_S / V_S$ and $\Delta V_P / V_P$ are (fractional) anisotropy for S-waves and P-waves, K_P and K_S are kernels derived as functions of surface wave eigenfunctions, ψ is azimuth and ψ_G is the azimuth of the fast velocity direction.

The azimuthally varying SV velocity variation in each layer is then expressed as

$$V_i = V_{0_i} + \Delta V_i \cos 2(\psi_i - \psi_{G_i}) \tag{5}$$

where following [Montagner and Griot-Pommera, 2000] ,

$$
\begin{aligned}
V_i &= V_{0_i} \left[1 + \frac{1}{2} \frac{G_{C_i}}{L_i} \cos 2\psi + \frac{1}{2} \frac{G_{S_i}}{L_i} \sin 2\psi_i \right] \\
&= V_{0_i} \left[1 + \frac{1}{2} \frac{G_i}{L_i} \cos 2(\psi_i - \psi_{G_i}) \right]
\end{aligned} \tag{6}
$$

and $G_i = \sqrt{G_{C_i}^2 + G_{S_i}^2}$, $\psi_{G_i} = \arctan(G_{S_i} / G_{C_i})$ and $G_{C_i} = G_i \cos 2\psi_{G_i}$, and $G_{S_i} = G_i \sin 2\psi_{G_i}$.

$$\frac{\Delta V_i}{V_{0_i}} = \frac{G_i}{L_i} \tag{7}$$

In order to convert to SKS splitting values we used Eq. (1) modified for a 4-layered structure becomes,

$$C = \sum_{i=1}^{4} \frac{G_{C_i}}{L_i} \frac{z_i}{V_{0_i}}; \quad S = \sum_{i=1}^{4} \frac{G_{S_i}}{L_i} \frac{z_i}{V_{0_i}} \tag{8}$$

with G_{C_i}/L_i, G_{S_i}/L_i obtained from the data using Eqs.(5), (6) and (7).

The results show that most significant splitting (80%) occurs in the mantle lithosphere layer ($i=3$), which is thickest and has largest anisotropy (Figure 2). Then Eq.(2) becomes

$$dt = \sqrt{\frac{\rho_3}{L_3}} \frac{\sqrt{G_{C_3}^2 + G_{S_3}^2}}{L_3} z_3$$

$$\phi_{fast} = \frac{1}{2} \text{atan}\left(\frac{G_{S_3}}{G_{C_3}}\right)$$

(9)

(Eq. (16) of Montagner and Griot-Pommera, 2000). That is, the splitting time is the fractional perturbation in travel time in layer 3 times the total travel time in that layer for vertically traveling S waves. Fast directions are found parallel to the SAF and reach maximum values to the south where the topography associated with the Transverse Ranges and Big Bend is largest. This appears to be an example of finite lithospheric strain, as it has the right direction and spatial distribution to associate it with lithospheric root effects caused by the mountain building (e.g., Kohler, 1999) but the directions and small delay times (on average 0.14 sec) cannot explain the SKS splitting (1.5 sec).

SKS Splitting

For the SKS splitting we analyzed all the data between 1990 and 2008. For each of the 235 seismic stations, all events (190 earthquakes, producing more than 33,000 seismograms) were visually inspected. We considered events with magnitude greater than 6.5 and epicentral distance greater than 90 and less than 120 degrees in order to avoid contamination by other S wave phases. For various reasons, such as noisy data, non-reporting stations, we found on average 53 events at 174 stations suitable for splitting analysis, i.e. a total of 8533 splitting measurements (Figure 1). The data were bandpass filtered with corner frequencies of 0.01 Hz and 1 Hz to improve signal to noise ratio. For

estimates of splitting parameters of individual events we used the method of Silver and Chan, [1991b]. For station averages we used the method of Davis [2003], simultaneously minimizing the energy of the transverse component of all suitable seismograms at a given station. Because splitting parameters from individual events are scattered, especially if they are polarized near null-directions, waveforms from multiple events are stacked, and the splitting operator applied to the composite waveform. This approach gives more robust results than averaging widely scattered individual estimates [Vinnik *et al.*, 1989; Wolfe and Silver, 1998] .

Results

SKS Splitting from Surface Wave Anisotropy

In southern California the SKS splitting fast directions exhibit a general WSW-ENE trend with apparent deflection at stations in the Transverse Ranges region (Figure 3). As we shall see, in northern California there is a change in direction across the SAF, taken to be near the plate boundary (Figure 7) but this is much more gradual in southern California.

SKS splitting parameters for the surface wave anisotropy model exhibit significant differences from those obtained from SKS/SKKS splitting (Figure 4). First of all, even the maximum delay time predicted by the surface model is 0.5 seconds, and on average 0.14 sec, much smaller than >1 second SKS splitting in this region. The fast axes directions are also different in that surface wave results are mostly parallel to the relative plate motion direction. Larger variations are observed closer to the SAF. The results suggest that at least two layers of anisotropy are required to explain the two data sets, the first in the depth range 33-100km and the second deeper.

We corrected the SKS and SKKS seismograms for anisotropy effects in the mantle lithosphere using the results from the surface wave analysis by rotating the east and west components into fast and slow directions, and advancing the phase of the slow component by the surface wave splitting time, and then rotating back to east and west. We tested this method using synthetics (See supplementary material). Then we invert the corrected data for SKS and SKKS splitting parameters. As can be seen in Figure 3 the anisotropy from the surface wave model has minor effects on the overall SKS pattern. After correction, fast directions rotate anticlockwise on average about 3 degrees, and delay times decrease by an average 0.1 sec. We therefore conclude that the anisotropic structure in the uppermost mantle (33-100 km), derived from surface waves, cannot explain SKS splitting. The correspondence of the surface wave fast directions with the strike and topography of the Transverse Ranges suggests it is probably related to the finite strain in the lithosphere from the transpression associated with the Big Bend. We also conclude that the SKS and SKKS phases are sensitive to the deeper parts of the upper mantle that are not sampled by the surface wave eigenfunctions, possibly down to 300-400 km [Becker *et al.*, 2006a; Becker *et al.*, 2006b]. We note a small crustal contribution of about 0.1-0.3 sec could be part of the total delay time [Boness and Zoback, 2006; Li *et al.*, 1994] but the surface wave analysis of crustal layers indicates it averages at the low end of that range.

Azimuthal Dependence of Splitting

We also carried out a systematic analysis of splitting parameters as a function of back azimuth. Splitting parameters from different events agreed in general, but we observed significant variations in splitting parameters at individual stations depending on event-back azimuth. Such behavior suggests a departure from the simplest model of a single anisotropic layer. Again, because limited numbers of events gave rise to scattered signals, we restricted the analysis to stations that had multiple events (#>3) in a given azimuth range (Figure 5a).

Only 14 stations satisfied these criteria, and the results are plotted in Figure 5b. Most of the stations on the northeast side of the SAF exhibit a systematic clockwise rotation (blue to red) of the fast directions by about 40° as azimuth rotates clockwise by 100°. However stations in the west and northwest have variable rotations. Silver and Savage, [1994] suggested that apparent splitting parameters are expected to show characteristic $\pi/4$ periodicity for two-layer anisotropy, but we did not observe this pattern in our data. Other possible explanations for azimuth-dependent splitting, are noise in the data, multi-layer splitting, a layer with dipping symmetry axis, or anisotropy caused by an inhomogeneous medium [Fouch and Rondenay, 2006]. Regional tomography [Kohler *et al.*, 2003] indicates the upper mantle is heterogeneous and rays from different azimuths may sample lateral variations in anisotropy. We tested whether anisotropy was dependent on event depth but found no correlation.

Comparison of Fast Directions with Absolute Plate Motions Relative to the Hot Spot Reference Frame

Splitting directions are found to correlate well with absolute plate motions relative to the hot spot reference frame [NUVEL 1A model, Gripp and Gordon, 2002] for most stations. Figure 6 shows splitting directions in southern California plotted with North American and Pacific absolute plate motion (APM) vectors. The correlation is excellent, suggesting the stacking method used has produced spatially robust directions, and that APM provides a good explanation for the fast-axes directions. However, on crossing the SAF we expect a rotation to Pacific plate motion, but other than at a few stations off the coast, the direction remains relatively constant.

We therefore extended the analysis to all stations of the California Integrated Seisimic Network (Figure 7 and Supplementary Table 1). Figure 7 shows that, if we approximate the plate boundary as the SAF, in northern and central California, there is indeed a transition in the fast-axes directions from parallel to the North American APM to the Pacific Plate APM. In southern California this correlation with APM agrees well in the east, but breaks down to the west. In the south it appears that if the plate boundary is the point where splitting rotates to Pacific APM, it is not at the San Andreas Fault but lies to the west of it. We estimate this notional boundary by finding a line where splitting either side makes the transition from North American to Pacific plate APM. We restricted the line to lie along the azimuth of relative plate motion, which for the NUVEL1A model is in a direction $N37^oW$, and found that it passes through a point of latitude 35°, and longitude 241°. This notional plate-boundary line lies east of the SAF in central and northern California but to the west in southern California. Since most of the SKS rays are from the east, deep anisotropy effects would project to the eastern side of the SAF. In Figure 8 we plot fast directions as a function of distance measured at right angles to the inferred plate boundary in southern (Figure 8a) and central-northern California (Figure 8b) fit to a smooth variation showing the transition from North American to Pacific plate motion is more apparent in the north.

Discussion

As mentioned in the introduction Wuestefeld et al., [2009] find a statistically significant correlation between splitting inferred from surface waves and SKS splitting for wavelengths > 600km. At the smaller scale in southern California (~300km) surface waves and splitting fast directions differ and appear to arise at different depths, probably generated by different processes. Wuestefeld *et al.*, [2009] regional analysis of western North America

shows good agreement between the surface wave and splitting fast directions. West North America has a complicated mantle flow that includes the superimposed effects of APM, the Yellowstone hot spot, and a transition from subduction to strike-slip tectonics to produce a complex toroidal mantle flow pattern (e.g., [Beghein *et al.*, 2009; Xue and Allen, 2007; Zandt and Humphreys, 2008]). However, most of central and southern California lies south of these lateral variations and, as we find here, the SKS splitting may be dominated by APM.

For southern California most previous studies have found that fast directions in SKS splitting measurements are dominantly ENE-WSW [Liu et al., 1995; Ozalaybey and Savage, 1995; Polet and Kanamori, 2002; Savage and Silver, 1993; Silver and Holt, 2002]. The fast direction in SKS splitting is most likely due to the strain-induced lattice-preferred orientation (LPO) of olivine. SKS splitting is usually associated with regions shallower than ~400 km, where most anisotropy seems to reside [Becker et al., 2006a; Becker et al., 2006b]. A pre-existing fossil anisotropy frozen in the lithosphere could be another possibility, but our surface wave analysis indicates that, while evidence for lithospheric anisotropy exists in the Big Bend region, it is small and negligible elsewhere. Becker et al. [2006b] obtain significant radial anisotropy from mantle flow modeling and Moschetti et al. [2010] observe the same in the area of this study. Both our surface wave and splitting measurements are not sensitive to radial anisotropy. We performed synthetic tests using layers with orthorhombic symmetry and different splitting parameters and concluded that radial anisotropy has a small second order effect that does not change the conclusions presented here (See supplementary material).

Since the lithospheric effects appear to be too small to explain the shear-wave splitting, we examine the effects of sub-lithospheric mantle flow. There are two different views of the dynamics of mantle flow for Western America. Silver and Holt, [2002] argue that the mantle flows due east in a hot spot reference frame, nearly opposite to the direction of North American plate motion (west-southwest). They suggest that the mantle flow in

western North America is weakly coupled to the motion of the surface plate, producing small drag force, and that this flow field is probably due to heterogeneity in mantle density that is produced by the sinking Farallon slab. On the other hand, Becker *et al.*, [2006b] suggest that coupling exists between the mantle flow and the North America plate. They conclude that the interaction between mantle and lithospheric motions need not be weak to explain splitting, implying potentially strong plate driving forces associated with mantle flow. Further to the north of our study area Zandt and Humphreys, [2008] suggest a circular pattern of fast directions seen in West North America is related to toroidal flow around the Juan de Fuca slab as it retreats west. While this may affect some our northern stations its affect is probably small in the Big Bend area of southern California.

In a study of Rayleigh wave azimuthal anisotropy beneath southern California, Yang and Forsyth, [2006] found that the anisotropy determined from long-period surface waves extends through both lithosphere and asthenosphere. They found that the strength of azimuthal anisotropy is ~1.7% at periods shorter than 100 s and less than 1% at longer periods. They also find that the fast direction is nearly E-W and the anisotropic layer is more than 300 km thick. Polet and Kanamori, [2002] used SKS splitting time to estimate an anisotropic layer about 100-200 km thick with assumption of 4% anisotropy for upper mantle material. Using estimates of long period P wave polarization, P_n times [Hearn, 1996], and Rayleigh and Love wave velocities, [Davis, 2003] concluded that anisotropy is distributed throughout the upper 200 km of the mantle up to the base of the crust.

In this study, which uses shorter periods than the Yang and Forsyth, [2006] study, we find that predicted surface wave splitting times obtain their largest values in the mantle lithosphere (velocity variations up to 1.5%), but are much less than SKS and SKKS splitting times. The surface wave fast axes directions are also different from SKS and are mostly parallel to the relative plate motion direction and major faults. The largest variations occur

just south of the Big Bend where transpression has been greatest. We correct the SKS and SKKS seismograms for anisotropy effects in the mantle lithosphere using the results from the surface wave analysis. After correction, fast directions only rotate anticlockwise on average about 3 degrees and delay times decrease by on average 0.1 sec. The overall SKS and SKKS pattern is hardly affected. Also, the larger splitting observed (~1-1.5s) requires an anisotropic layer that is thicker than the mantle lithosphere. Therefore we conclude anisotropic structure derived from surface waves clearly cannot explain SKS splitting data, but is probably related to the finite strain from the plate tectonics. We suggest that the SKS and SKKS phases are sensitive to the deeper parts of the upper mantle, and given the correlation with APM it is probably located in the asthenosphere.

Polet and Kanamori, [2002] plotted the fast directions of anisotropy and the maximum compressive stress directions from the world Stress Map together for southern California. They found that the fast direction is nearly orthogonal to the maximum compressive stress, and argued that this perpendicularity is consistent with the alignment of the a–axis of olivine perpendicular to the direction of lithospheric shortening. This mechanism, however, does not explain the larger contribution to splitting from the asthenosphere, which is unlikely to be directly coupled to any lithospheric shortening.

Given the good correlation between absolute plate motion in central and northern California, and on the eastern side of southern California, we suggest the shear-wave splitting is due to drag on the asthenosphere by the absolute plate motion of the over-riding plates. However, in west-southern California the effect of the Big Bend causes the plate margin to be much more diffuse than further north. This contrast south to north, across the Big Bend, extends to Baja California where splitting analyses have obtained similar E-W fast directions to those in southern California [Obrebski *et al.*, 2006; Obrebski and Castro, 2008]. We suggest that the mantle flow models (e.g., [Becker *et al.*, 2007a; Becker *et al.*, 2007b; Silver

and Holt, 2002]) are unlikely to have a sudden change across the Big Bend, and that the difference is due to the history of the plate tectonic interactions. Prior to 30 Ma, when the east Pacific rise collided with North America, most of the region west of the SAF had North American plate motion. With the collision, and development of the transpressive plate boundary, parts of North America were captured and have taken on Pacific plate motion [Atwater and Menard, 1970]. North of the Big Bend the relative motion across the plate boundary has concentrated near the SAF and nearby offshore faults such as the San Gregorio and Hosgri Faults. Over the last 12 Ma the relative plate displacement is as much as 400-500 km [Powell *et al.*, 1994] across a narrow boundary region that GPS measurements show continues narrow to the present.

South of the Big Bend the relative displacement has been, and continues to be, broadly distributed. Over the past 12 Ma the transform motion has stepped east from offshore to the San Gabriel Fault, and then at 5 Ma to the SAF, which has an offset of just 160-180 km [Powell *et al.*, 1994]. The plate capture has involved microplate capture in the continental borderland with significant motion offshore. Thus the underlying asthenosphere beneath onshore stations has seen less accumulated Pacific plate APM.

It takes more than 40% finite strain to overprint a previous anisotropy [Ribe, 1992]. We explain the Big Bend contrast in southern California as due to fact that the Pacific Plate motion for captured North America, southwest of the Big Bend, has been insufficient to overprint North American APM. This has been more successful in central and northern California where the finite strain is estimated to be more than a factor of two larger. We expect that offshore, both southern and northern California, the anisotropy will rotate to be fully parallel to Pacific plate APM (Figure 8), some indication of which is apparent in global surface wave anisotropy maps [Montagner and Griot-Pommera, 2000; Montagner and

Guillot, 2000; Wuestefeld *et al.*, 2009]. Given the small anisotropy in layer 4 (100-150 km) and the apparent correlation with the history of APM, we suggest the shear zone beneath the plate and the lower mantle is distributed over about 400 km and not concentrated in the low velocity asthenosphere that surface waves indicate lies at a depth of about 70 to 100 km.

Conclusions

The combined SKS and surface wave splitting results can explain earlier estimates of azimuthal anisotropy from P_n that found SAF-aligned directions [Hearn, 1984; Smith and Ekstrom, 1999; Sung and Jackson, 1992] in southern California. In this region, the Rayleigh wave fast directions N112^{o}W are in agreement with previous studies of P_n anisotropy which vary from N115E [Sung and Jackson, 1992] to ~N120^{o}E [Smith and Ekstrom, 1999]. Both surface waves and P_n are sensitive to uppermost mantle structures. But surface wave and P_n results are in stark contrast with the fast SKS splitting directions N80^{o}E suggesting anisotropy twists anticlockwise with depth. SKS Splitting values, which have been corrected for mantle lithosphere effects, are remarkably parallel to plate motions. This suggests that transpression that has given rise to the San Gabriel Mountains in the Big Bend region has generated anisotropy in the mantle lithosphere, but deeper down, absolute plate motion aligns olivines in the asthenosphere. Given the small anisotropy observed in the longest period surface waves (<2%) and the correlation of splitting with absolute plate motions it appears that the zone of finite shear between absolute plate motion and the deeper mantle is distributed much deeper (down to 300-400 km) than previously thought.

References

Alvizuri, C. and T. Tanimoto, Azimuthal anisotropy from array analysis of Rayleigh waves in Southern California, submitted to Geophys. J. Int., 2011.

Alvizuri, C. and T. Tanimoto, Observations of Surface Wave Azimuthal Anisotropy in Southern California by Direct Application of the Beamforming Method, abstract, AGU Fall Meeting, DI13A-1842, 2010.

Atwater, T., and H. W. Menard (1970), Magnetic Lineations in Northeast Pacific, Earth and Planetary Science Letters, 7(5), 445-450.

Becker, T., et al. (2006a), Statistical properties of seismic anisotropy predicted by upper mantle geodynamic models, in J. Geophys. Res.,-Solid Earth, VOL. 111, B08309, doi:10.1029/2005JB004095.

Becker, T., et al. (2006b), Mantle flow under the western United States from shear wave splitting, in Earth and Planetary Science Letters, 247,235–251.

Becker, T., et al. (2007a), Length scales, patterns and origin of azimuthal seismic anisotropy in the upper mantle as mapped by Rayleigh waves, in Geophys. J. Int., 171, 451-462.

Becker, T. W. (2006), On the effect of temperature and strain-rate dependent viscosity on global mantle flow, net rotation, and plate-driving forces, Geophys. J. Int., 167(2), 943-957.

Becker, T. W., et al. (2007b), Stochastic analysis of shear-wave splitting length scales, Earth and Planetary Science Letters, 259(3-4), 526-540.

Beghein, C., et al. (2009), Depth Constraints on Azimuthal Anisotropy in the Great Basin from Rayleigh Wave Phase Velocity Maps in Earth and Planetary Science Letters, edited, pp. 1-54.

Boness, N. L., and M. D. Zoback (2006), Mapping stress and structurally controlled crustal shear velocity anisotropy in California, Geology, 34(10), 825-828.
Crampin, S., et al. (1986), Shear-Wave Polarizations in the Peter-the-First Range Indicating Crack-Induced Anisotropy in a Thrust-Fault Regime, Geophysical Journal of the Royal Astronomical Society, 84(2), 401-412.

Davis, P. (2003), Azimuthal variation in seismic anisotropy of the southern California uppermost mantle, J. Geophys. Res.,-Solid Earth, NO. B1, 2052, doi:10.1029/2001JB000637.

Fouch, M., and S. Rondenay (2006), Seismic anisotropy beneath stable continental interiors, Physics of the Earth and Planetary Interiors, 158, 292-320.

Gripp, A. E., and R. G. Gordon (2002), Young tracks of hotspots and current plate velocities, Geophys. J. Int., 150(2), 321-361.

Hearn, T. M. (1984), Pn Travel-Times in Southern-California, J. Geophys. Res.,, 89(NB3), 1843-1855.

Hearn, T. M. (1996), Anisotropic Pn tomography in the western United States, J. Geophys. Res.,-Solid Earth, 101(B4), 8403-8414.

Karato, S., et al. (1989), Seismic anisotropy; mechanisms and tectonic implications, in Rheology of solids and of the Earth., edited, pp. 393-422.

Karato, S., (2006), Influence of hydrogen-related defects on the electrical conductivity and plastic deformation of mantle minerals: A critical review, In "Earth's Deep Water Cycle" (eds. S.D. Jacobsen and S. van der Lee), American Geophysical Union, Washington DC, 113-129.

Keith, C. M., and S. Crampin (1977a), Seismic body waves in anisotropic media: reflection and refraction at a plane interface, Geophys. J. R. Astron. Soc., 49, 181 – 208.

Keith, C. M., and S. Crampin (1977b), Seismic body waves in anisotropic media: synthetic seismograms, Geophys. J. R. Astron. Soc., 49, 225 – 243.

Kohler, M. D., (1999), Lithospheric deformation beneath the San Gabriel Mountains in the Southern California Transverse Ranges, J. Geophys. Res., 104, 15025-15041.

Kohler, M. D., et al. (2003), Mantle heterogeneities and the SCEC reference three-dimensional seismic velocity model version 3, Bull. Seism. Soc. Amer., 93(2), 757-774.

Kosarev, G., et al. (1984), Anisotropy of the mantle inferred from observations of P to S converted waves, Geophysical Journal of the Royal Astronomical Society, 76(1), 209-220.

Li, Y. G., et al. (1994), Shear-Wave Splitting Observations in the Northern Los-Angeles Basin, Southern California, Bull. Seism. Soc. Amer., 84(2), 307-323.

Liu, H., et al. (1995), Sks Splitting beneath Southern California, Geophysical Research Letters, 22(7), 767-770.

Makeyeva, L. I., et al. (1992), Shear-Wave Splitting and Small-Scale Convection in the Continental Upper Mantle, Nature, 358(6382), 144-147.

Montagner, J. P., and T. Tanimoto (1991), Global Upper Mantle Tomography of Seismic Velocities and Anisotropies, J. Geophys. Res.,-Solid Earth, 96(B12), 20337-20351.

Montagner, J. P. (1994), Can seismology tell us anything about convection in the mantle, Reviews of Geophysics, 32(2), 115-137.

Montagner, J. P. (1998), Where can seismic anisotropy be detected in the earth's mantle? In boundary layers in Pure Appl. Geophys. 151, 223-256.

Montagner, J. P., and D-A Griot-Pommera. (2000), How to relate body wave and surface wave anisotropy?, J. Geophys. Res.,-Solid Earth, 105(B8), 19015-19027.

Montagner, J. P., and L. Guillot (2000), Seismic anisotropy tomography Problems in Geophysics for the Next Millennium, Boschi E., Ekstrom G., Morelli A. (eds) Editrice Compositori, Bologna, Italy , 217-254.

Moschetti, M. P., et al., (2010), Seismic evidence for widespread western-US deep-crustal deformation caused by extension, Nature 464, 885-889, doi:10.1038/nature08951.

Nicolas, A., et al. (1987), Formation of anisotropy in upper mantle peridotites: A review, in Composition, Structure, and Dynamics of the Lithosphere-Asthenosphere System, Geodyn. Ser., edited, pp. 111-123.

Obrebski, M., et al. (2006), Shear-wave splitting observations at the regions of northern Baja California and southern Basin and Range in Mexico, Geophysical Research Letters, 33, L05302, doi:10.1029/2005GL024720.

Obrebski, M., and R. R. Castro (2008), Seismic anisotropy in northern and central Gulf of California region, Mexico, from teleseismic receiver functions and new evidence of possible plate capture, J. Geophys. Res., 113, B03301, doi:10.1029/2007JB005156.

Okaya, D., and T. McEvilly, (2003), Elastic wave propagation in anisotropic crustal material possessing arbitrary internal tilt, Geophys. J. Int., 153, 344-358.

Ozalaybey, S., and M. K. Savage (1995), Shear-Wave Splitting beneath Western United-States in Relation to Plate-Tectonics, J. Geophys. Res.,-Solid Earth, 100(B9), 18135-18149.

Polet, J., and H. Kanamori (2002), Anisotropy beneath California: shear wave splitting measurements using a dense broadband array, Geophys. J. Int., 149(2), 313-327.

Powell, R. E., et al. (1994), The San Andreas fault: A balance palinspastic reconstruction and geologic evolution, Geological Society of America, 178.

Prindle, K., and T. Tanimoto (2006), Teleseismic surface wave study for S-wave velocity structure under an array: Southern California, Geophys. J. Int., 166(2), 601-621.

Ribe, N. M. (1992), On the Relation between Seismic Anisotropy and Finite Strain, J. Geophys. Res.,-Solid Earth, 97(B6), 8737-8747.

Savage, M. K., and P. G. Silver (1993), Mantle deformation and tectonics: constraints from seismic anisotropy in the western United-States, Physics of the Earth and Planetary Interiors, 78(3-4), 207-227.

Savage, M. K. (1999), Seismic anisotropy and mantle deformation: What have we learned from shear wave splitting?, Reviews of Geophysics, 37(1), 65-106.

Silver, P. G., and W. W. Chan (1991a), Shear wave splitting and subcontinental mantle deformation, J. Geophys. Res., 96(B10), 16,429-416,454.

Silver, P. G., and W. W. Chan (1991b), Shear-Wave Splitting And Subcontinental Mantle Deformation, J. Geophys. Res.,-Solid Earth, 96(B10), 16429-16454.

Silver, P. G., and M. K. Savage (1994), The Interpretation of Shear-Wave Splitting Parameters in the Presence of 2 Anisotropic Layers, Geophys. J. Int., 119(3), 949-963.

Silver, P. G. (1996), Seismic anisotropy beneath the continents: Probing the depths of geology, Annual Rev. Earth Planet. Sci., 24, 385-432.

Silver, P. G., and W. E. Holt (2002), The mantle flow field beneath western North America, Science, 295(5557), 1054-1057.

Smith, G. P., and G. Ekstrom (1999), A global study of P-n anisotropy beneath continents, J. Geophys. Res.,-Solid Earth, 104(B1), 963-980.

Sung, L., and D. Jackson (1992), Crustal and uppermost mantle structure under southern California, Bull. Seism. Soc. Amer., 82, 934–961.

Tanimoto, T., and K. Prindle (2007), Surface wave analysis with beamforming, Earth Planets and Space, 59(5), 453-458.

Vinnik, L. P., et al. (1989), Azimuthal Anisotropy in the Lithosphere from Observations of Long-Period S-Waves, Geophys. J. Int., 99(3), 549-559.

Wolfe, C. J., and P. G. Silver (1998), Seismic anisotropy of oceanic upper mantle: Shear wave splitting methodologies and observations (vol 103, pg 749, 1998), J. Geophys. Res.,-Solid Earth, 103(B2), 2791-2791.

Wuestefeld, A., et al. (2009), Identifying global seismic anisotropy patterns by correlating shear-wave splitting and surface-wave data, Physics of the Earth and Planetary Interiors, 176(3-4), 198-212.

Xue, M., and R. A. Allen (2007), The fate of the Juan de Fuca plate: Implications for a Yellowstone plume head, in Earth and Planetary Science Letters, edited, pp. 266-276.

Yang, Y., and D. Forsyth (2006), Regional tomographic inversion of amplitude and phase of Rayleigh waves with 2-D sensitivity kernels, Geophys. J. Int., 166, 1148-1160.

Zandt, G., and E. Humphreys (2008), Toroidal mantle flow through the western U.S. slab window, Geol, 36(4), 295.

Figure 1: Location of earthquakes (red dots) used for analysis in this study. Each circle shows 30-degree distance. Magnitude of events are Mw >6.5.

Figure 2A. Calculated splitting times from surface wave analyses from mantle lithosphere (33 -100 km). The other layers give negligible effects. The surface waves fast axes are parallel to the San Andreas Fault (curved dark line) and obtain maximum values south of the fault, in the region of high topography associated with the Big Bend.

Figure 2B. A cross-section showing that splitting along the line in Figure 2A. The maximum anisotropy occurs just south of the San Andreas Fault in the Transverse Ranges.

Figure 3. SKS splitting for stacked data 1990-2008. Black and red lines give fast directions before and after correction for splitting in the upper 100 km of the mantle as determined from surface waves. Apart form some anticlockwise rotations in the Transverse Ranges the differences are very small, suggesting the largest splitting occurs at greater depths.

Figure 4. Contrast between splitting determined from the surface wave data (red lines) with the SKS splitting results (black lines). The splitting results have been corrected for the effects of the upper 33-100 km of the mantle and show a general parallelism WSW-ENE. The plot shows that the surface wave anisotropy neither matches the direction or amplitudes of the SKS data.

Figure 5A SKS splitting times and fast directions as a function of back azimuth of arriving waves. Rotation of the easternmost stations may be due to variable anisotropy with depth. It is not explained by the upper 100 km anisotropy as determined from surface waves.

Figure 5B. Stations that have multiple events (#>3) in a given azimuth range. SKS splitting times and fast directions as a function of back azimuth of arriving waves for 14 stations.
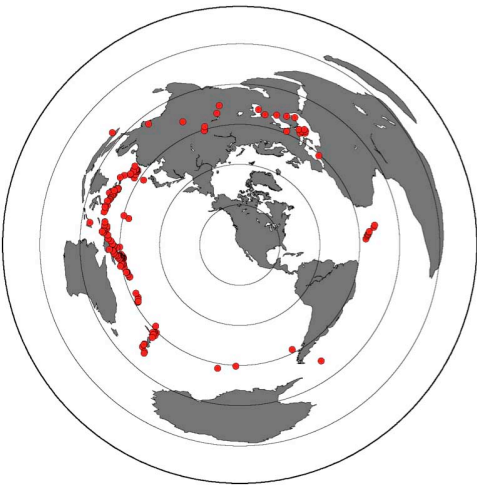
Figure 6. Comparison between the direction of absolute plate motion (APM) of the North American plate (red lines) and the splitting variations of the SKS phase (black lines). Except for a few stations in the west the correlation with APM is excellent.

Figure 7. Comparison between APM and splitting variations of the SKS phase for California Stations. Yellow lines give Pacific plate APM from the Nuvel 1A model [Gripp and Gordon, 2002]. Red lines denote North American APM and black lines are SKS splitting fast directions. The brown box shows stations that have splitting directions that are rotated towards Pacific plate APM consistent with the 400-500 km of relative motion across the San Andreas Fault system that has occurred after plate capture. In southwestern California the onshore relative motion west of the SAF has been less than half this amount, insufficient to rotate the fast directions.
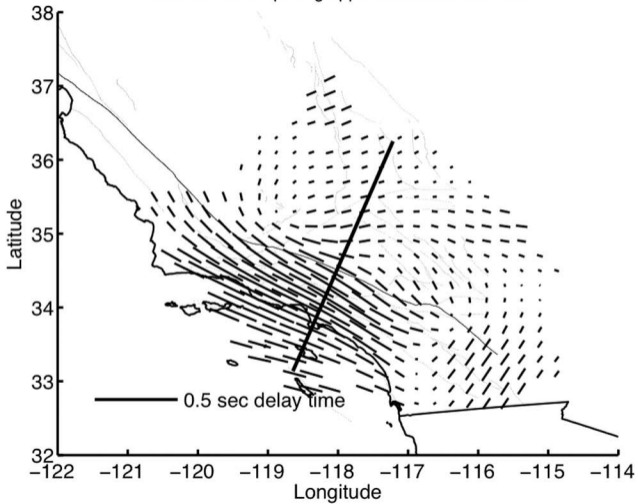
Figure 8a: Central and Northern California variations of SKS azimuth as function of distance from ref. plate boundary between North America plate and Pacific plate.
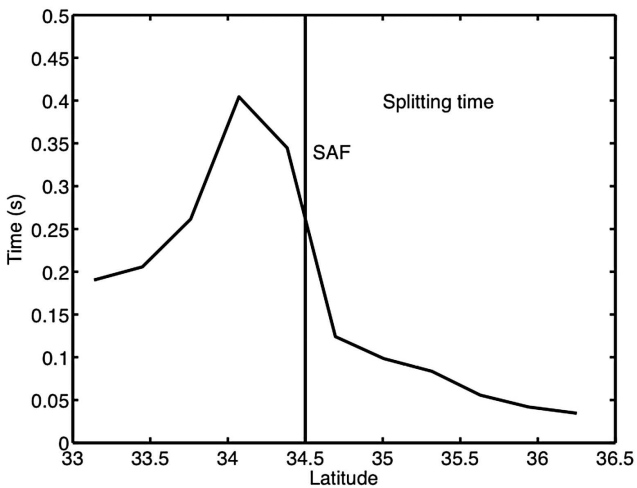
Figure 8b: Southern California variations of SKS azimuth as function of distance from inferred plate boundary between North America plate and Pacific plate.
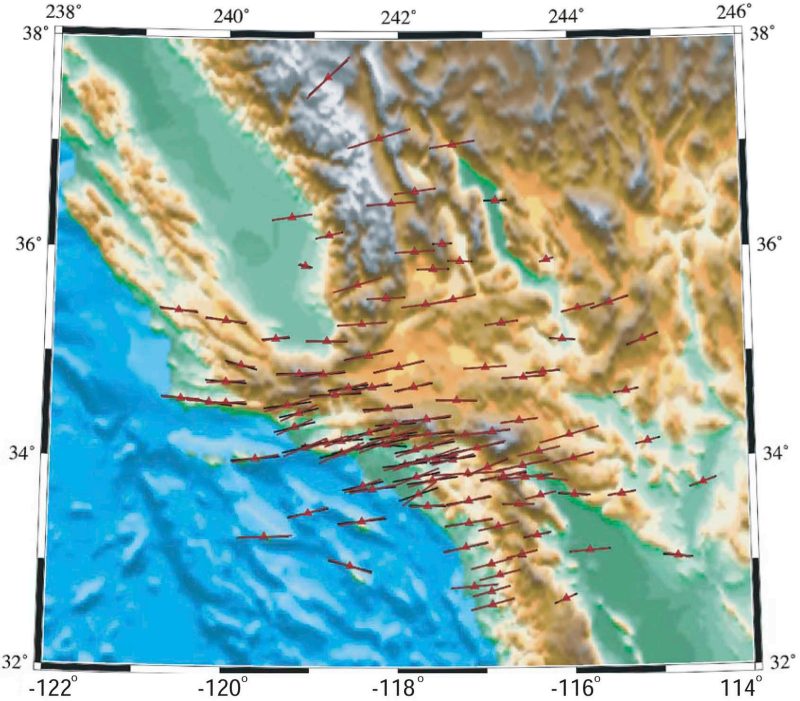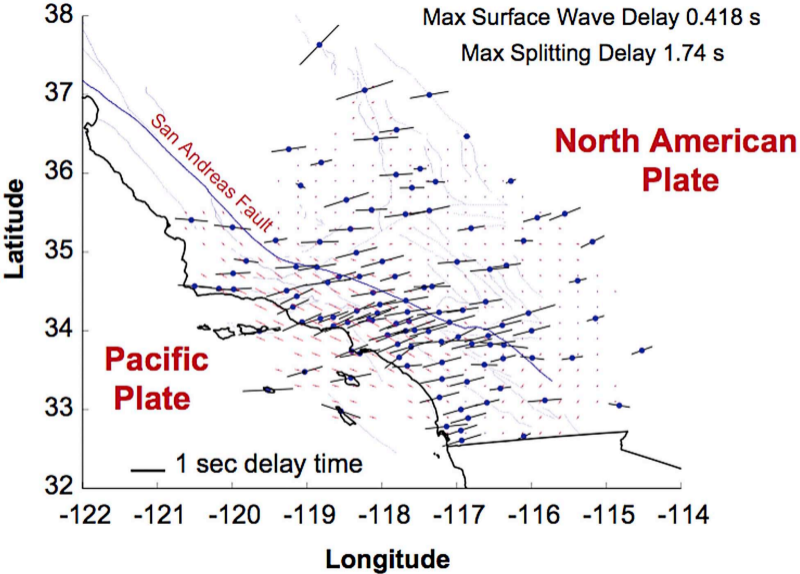
Location of Events

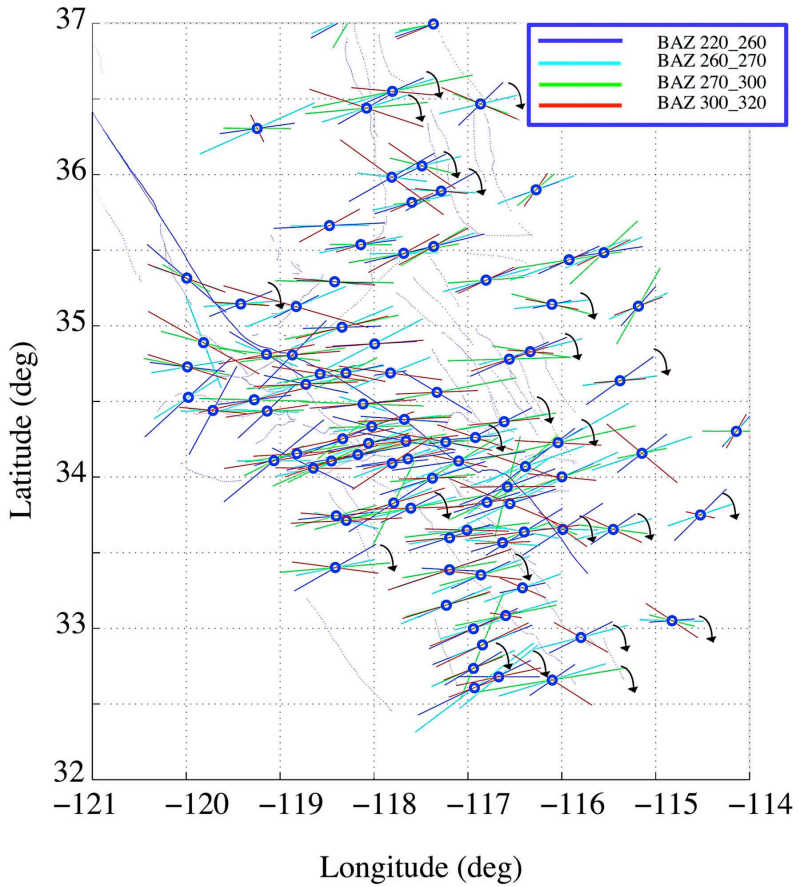Surface wave splitting upper mantle 33–100 km

Max Surface Wave Delay 0.418 s

Max Splitting Delay 1.74 s

North American Plate

San Andreas Fault

Pacific Plate

1 sec delay time

SKS–SKKS Splitting

BAZ 220_260
BAZ 260_270
BAZ 270_300
BAZ 300_320

SKS Splitting
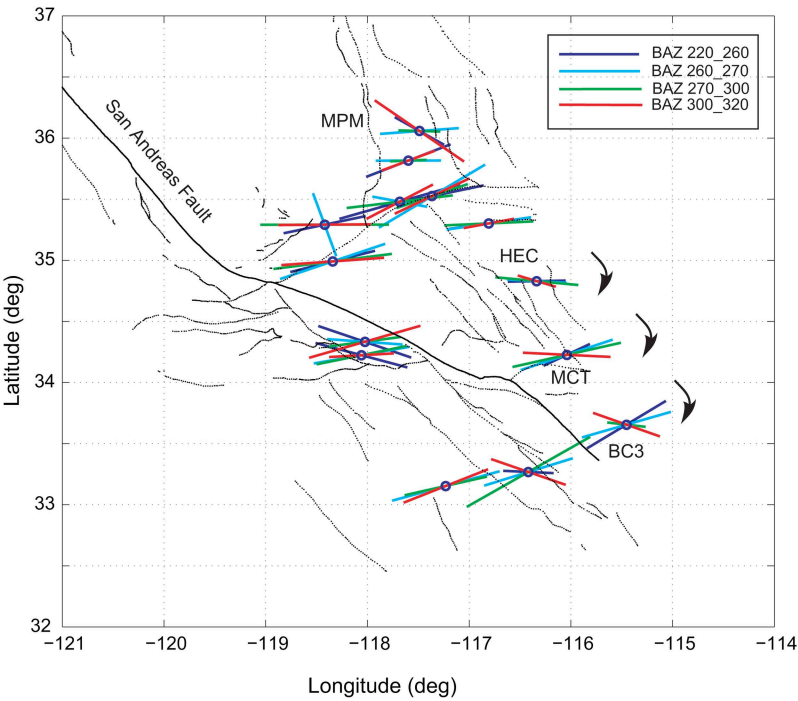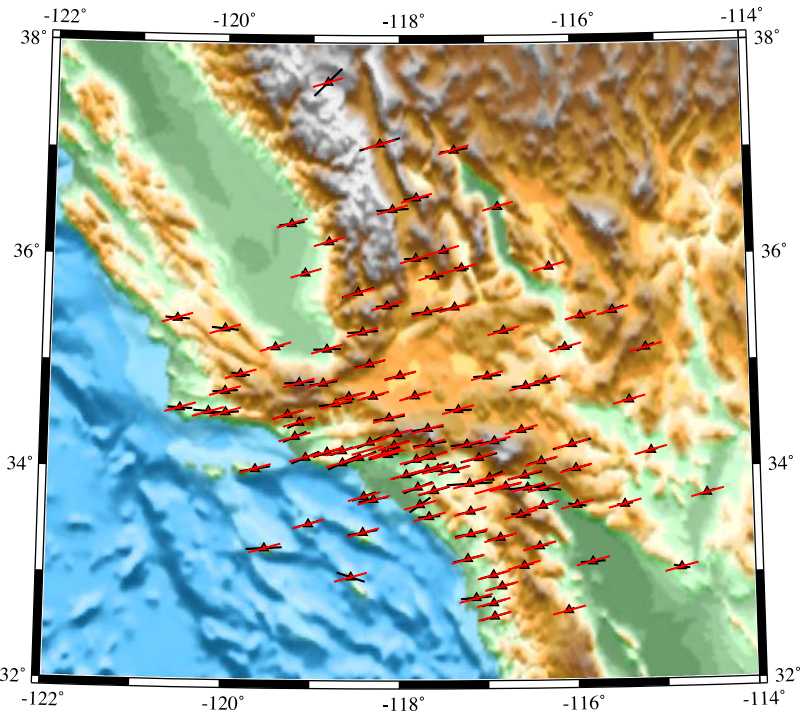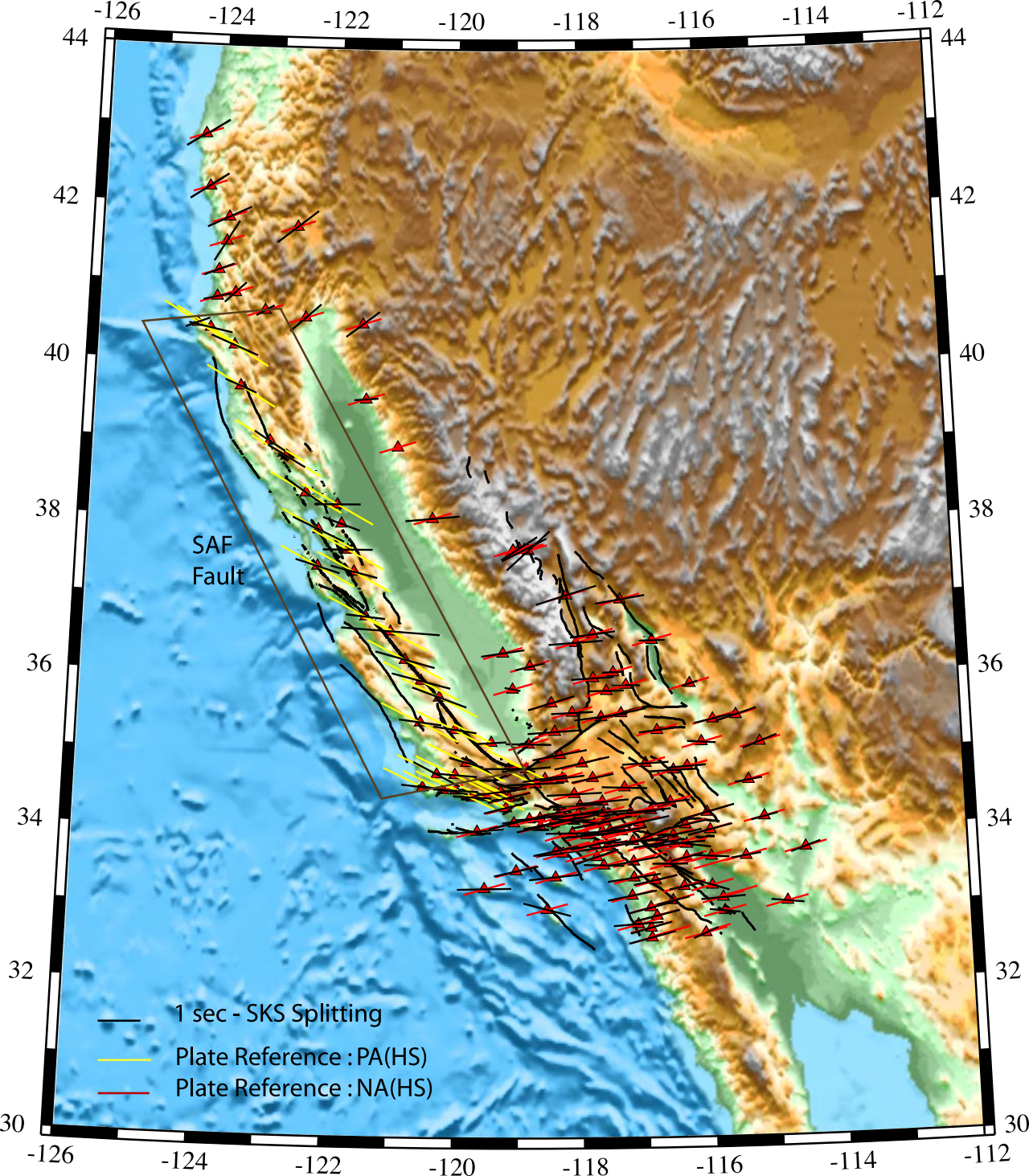
Plate Reference: North America
speed: 30-33 mm/yr, Azimuth:251-254

SAF
Fault

1 sec - SKS Splitting
Plate Reference : PA(HS)
Plate Reference : NA(HS)

North of Big Bend

PA   mean fast direction = 104°
NAM mean fast direction = 74°

South of Big Bend

PA   mean fast direction = 87°
NAM mean fast direction = 81°